

Crystal Structure of Form II of Syndiotactic Poly(1-butene)

Claudio De Rosa* and Domenico Scaldarella

Dipartimento di Chimica, Università di Napoli Federico II, Via Mezzocannone 4, 80134 Napoli, Italy

Received January 30, 1997; Revised Manuscript Received May 2, 1997

ABSTRACT: The crystal structure of form II of syndiotactic poly(1-butene) is presented. According to the present analysis, chains having a $s(5/3)2$ helical conformation are packed in a monoclinic unit cell with axes $a = 15.45$ Å, $b = 14.36$ Å, and $c = 20$ Å and with $\gamma = 116^\circ$. The crystalline density is 0.933 g/cm³ with four chains in the unit cell (40 monomeric units); the space group is $P2_1/a$.

Introduction

The polymorphism of syndiotactic poly(1-butene) (s-PB) has been recently described.¹ Two different crystalline modifications, form I and form II, have been found so far.

The crystallization of s-PB is a very slow process; indeed, by cooling from the melt or by precipitation or casting from polymer solutions, amorphous samples are generally obtained.¹ However, crystallization in form I occurs if amorphous samples are maintained at room temperature for several days.¹

The crystal structure of form I has been recently determined.² Form I is characterized by chains in $(TTGG)_2$ helical conformation with $s(2/1)2$ line repetition symmetry and identity period $c = 7.73$ Å.¹ The chains are packed in an orthorhombic unit cell with axes $a = 16.81$ Å, $b = 6.06$ Å, and $c = 7.73$ Å.² The space group proposed for the limit ordered structure, in which all the helical chains are isochiral, is $C22_1$.² The presence of some degree of disorder corresponding to the departure from the fully isochiral packing of the helices has been suggested.²

It is worth noting that the side groups of $s(2/1)2$ helical chains of form I are in an unusual "double" *gauche* conformation, that is the lateral methyl carbons are in a *gauche* arrangement with respect to both adjacent backbone methylene carbons. This was found by X-ray diffraction² and conformational energy calculations,¹ and was recently confirmed by the analysis of the solid state ¹³C NMR CP-MAS spectrum of form I.³

Form II of s-PB was obtained in stretched samples (generally together with form I), drawn at high draw ratio.¹ It is characterized by chains in a helical conformation of the kind $(TTGG)_n$ with $s(5/3)2$ symmetry and identity period $c = 20$ Å.¹ In the chains of form II the lateral methyl carbons are in the *trans* conformation with respect to one of two adjacent backbone methylene carbons and in the *gauche* conformation with respect to the other.¹

In this paper a detailed crystal structure of form II of s-PB is reported on the basis of packing energy calculations and a comparison between X-ray diffraction intensities and calculated structure factors.

Experimental Part and Method of Calculations

The s-PB sample was supplied by Montell. The polymer was synthesized with a homogeneous metallocene/methylaluminoxane catalytic system.⁴ The amount of *rrrr* pentads is equal to 93%.

Oriented fibers of s-PB in form II were obtained by performing the following procedure. Compression molded amorphous samples of s-PB were kept at low temperature (8–10 °C) in order to slow down the crystallization rate; the samples were stretched at room temperature at a high draw ratio ($\approx 700\%$) with a high draw rate (≈ 10 cm/s), just before the beginning of the crystallization in form I. The stretched samples were then kept at room temperature for several days so slow crystallization in oriented fibers of form II occurs. Fibers with a mixture of crystals of forms I and II are generally obtained. However this procedure allows us to reduce the crystallization in form I. The percentage of crystals in form II is higher than that obtained in the previous paper.¹

Wide angle X-ray fiber diffraction patterns were obtained with nickel-filtered Cu K α radiation by using a photographic cylindrical camera.

Calculated structure factors were obtained as $F_c = (\sum |F_i|^2 \cdot M_i)^{1/2}$, where M_i is the multiplicity factor and the summation is taken over all reflections included in the 2θ range of the corresponding diffraction spot observed in the X-ray fiber diffraction pattern. Only the values greater than the observable limit are reported. A thermal factor $B = 8$ Å² and the atomic scattering factors as in ref 5 were assumed. The observed structure factors, F_o , were evaluated from the intensities of the reflections observed in the X-ray fiber diffraction pattern, $F_o = (I_o/LP)^{1/2}$, where LP is the Lorentz-polarization factor for X-ray fiber diffraction: $LP = (1 + \cos^2 2\theta)/[2(\sin^2 2\theta - \zeta^2)^{1/2}]$. The experimental intensities I_o were observed by the multiple-film method and measured visually with an intensity scale.

The packing energy was evaluated as half the sum of the interaction energies between the atoms of one monomeric unit and all the surrounding atoms of neighboring macromolecules. The calculations were performed with the same function as used for the calculations of the conformational energy given elsewhere,¹ i.e. with the constants reported by Flory et al.⁶ and taking the methyl groups as a single rigid unit.⁷ The conformation of the chain, and hence the c axis, was kept constant, and the interactions were calculated within spheres of twice the sum of the van der Waals radii for each pair of atoms.

Results and Discussion

The X-ray fiber diffraction pattern of an oriented sample of s-PB essentially in form II is shown in Figure 1. The reflections showing good orientation arise from crystals of form II, whereas those showing bad orientation arise from crystals of form I. A comparison with the X-ray fiber diffraction pattern of form I, reported in ref 2, allows us to recognize the reflections of form I. All reflections of form II observed in the fiber pattern of Figure 1 are listed in Table 1.

As shown earlier,¹ these data are consistent with a helical conformation of the chains of the kind $(TTGG)_n$ with $s(5/3)2$ symmetry, in which the chain repetition ($c = 20$ Å) occurs after 5 conformational repeating units⁸

* Abstract published in *Advance ACS Abstracts*, June 15, 1997.

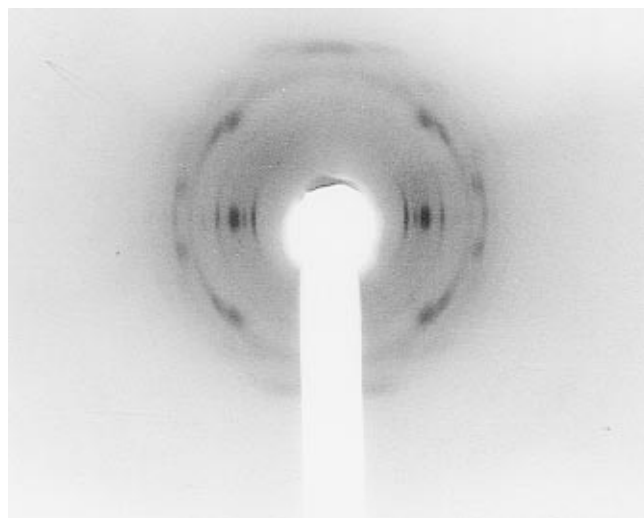


Figure 1. X-ray fiber diffraction pattern of form II of s-PB. Some reflections of form I are also present. These reflections can be easily recognized because they show bad orientation.

Table 1. Diffraction Angles 2θ , Bragg Distances d , Reciprocal Coordinates ξ and ζ , and Intensities I_{obs} , of the Reflections Observed on the Layer Lines l in the X-ray Fiber Diffraction Pattern of Form II of s-PB of Figure 1

2θ (deg)	d (Å)	ξ (Å ⁻¹)	ζ (Å ⁻¹)	l	I_{obs}^a
11.7	7.56	0.132	0	0	w
12.75	6.94	0.144	0	0	s
13.75	6.44	0.155	0	0	s
17.5	5.07	0.197	0	0	vw
22.7	3.92	0.255	0	0	vw
25.0	3.56	0.281	0	0	vw
20.6	4.31	0.226	0.0508	1	m
21.5	4.13	0.236	0.0508	1	m
22.3	3.99	0.230	0.101	2	vw
18.3	4.85	0.146	0.146	3	s
20.5	4.33	0.120	0.197	4	w
22.1	4.02	0.152	0.197	4	w
23.3	3.82	0.173	0.197	4	w
23.15	3.84	≈ 0	0.255	5	s

^a s = strong, m = medium, w = weak, vw = very weak.

(10 monomeric units) and after 3 turns around the chain axis. According to the previous analyses,¹ the values of the torsion angles along the main chain of form II, for the $s(5/3)2$ conformation, are $\theta_1 = 74^\circ$ and $\theta_2 = 196.5^\circ$, if the valence angles τ_1 and τ_2 are assumed to be 113° and 111° , respectively (C–C bond length = 1.54 Å), while the value of the torsion angle around the lateral groups is $\theta_3 = 180^\circ$. The definitions of the bond and torsion angles are shown in Figure 2.

It is worth noting that the formation of $s(M/N)$ complex helical symmetry with M and N not corresponding to very small integers is a consequence of the bulkiness of the lateral groups⁹ and corresponds to isodistortions for θ_1 and θ_2 from the exact *gauche* and *trans* values, as already found for various isotactic polymers.¹⁰ For syndiotactic polymers the isodistortion of the torsion angles and the formation of complex helical symmetries have been observed for poly(4-methyl-1-pentene).^{11,12}

The reflections observed in the X-ray fiber pattern of form II are all accounted for by a monoclinic unit cell with axes $a = 15.45$ Å, $b = 14.36$ Å, and $c = 20$ Å and with $\gamma = 116^\circ$. The calculated density, with four chains in the cell, is 0.933 g/cm³, in accordance with the experimental value (0.90 g/cm³ measured at 25°C by flotation for a sample with X-ray crystallinity close to 60%).

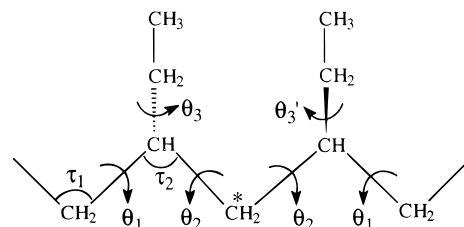


Figure 2. Definition of the torsion angles θ_1 , θ_2 , and θ_3 and the valence angles τ_1 and τ_2 . The torsion angles which characterize the conformations of the lateral groups in the conformational repeating units (θ_3 , θ_3') are defined with respect to the same CH_2 group (indicated by an asterisk). The binary axis, crossing the CH_2 groups of the main chain, for the $s(5/3)2$ symmetry, imposes the condition $\theta_3 = \theta_3'$.

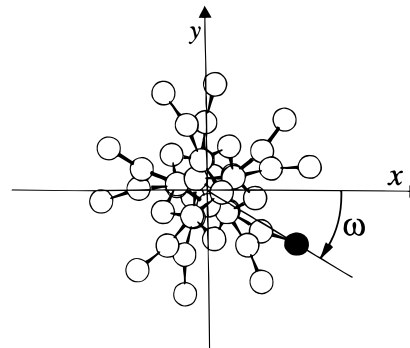


Figure 3. Definitions of the variables ω and z used in the packing energy map. The value of ω is positive for a clockwise rotation, and z is the height of the methyl carbon indicated as a filled circle.

The indexing of the observed reflections indicates the systematic absence of $hk0$ reflections with $h = 2n + 1$. The space group which is compatible with the presence of four chains in the cell and with the cited systematic absences is $P2_1/a$.

In order to find the best position of the chains inside the unit cell, calculations of the packing energy were performed for the space group $P2_1/a$. The position of the chain axis inside the unit cell was fixed at the fractional coordinates $x/a = 0$, $y/b = 0.25$, or $x/a = y/b = 0.25$, so that the lattice energy was calculated whilst maintaining the axes of the unit cell constant and varying only two parameters: the orientation of the chain around its axis (represented by the angle ω defined in Figure 3) and the z coordinate that defines the relative heights of the chains in the unit cell.

Maps of the packing energy as a function of ω and z , for the space group $P2_1/a$, with the chain axis at fixed positions $x/a = 0$, $y/b = 0.25$, and $x/a = y/b = 0.25$, are reported in Figures 4 and 5, respectively. The maps are periodic over $\omega = 180^\circ$ and $z = c/2 = 10$ Å, so only the regions with $\omega = 0-180^\circ$ and $z = 0-10$ Å are shown.

It is apparent that each map presents several equivalent energy minima; indeed, every minimum repeats identically after a rotation of $\omega = |180^\circ - t| = 36^\circ$, where t is the unit twist ($t = 360(3/5) = 216^\circ$), and a translation of $z = h = c/5 = 4$ Å, where h is the unit height. The minima of the map of Figure 5 have energies higher than those of the map of Figure 4. Starting from the minima of the maps, the packing energy has been minimized by varying all parameters ω , x , y , and z . After these minimizations, all minima have similar values of the energy. The deepest minimum is obtained in the case of Figure 4, when the chain axis is in the position $x/a \approx 0$, $y/b \approx 0.25$. The minima obtained in the case of

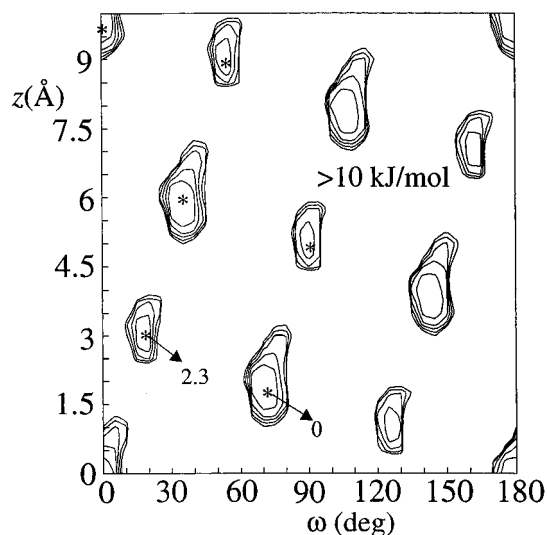


Figure 4. Map of the packing energy as a function of ω and z for the monoclinic unit cell with axes $a = 15.45$ Å, $b = 14.36$ Å, and $c = 20$ Å and with $\gamma = 116^\circ$ and space group $P2_1/a$, with the chain axis fixed at the position $x/a = 0$, $y/b = 0.25$. The curves are drawn at intervals of 2 kJ/(mol of monomeric unit) with respect to the absolute minimum of the map, assumed as zero.

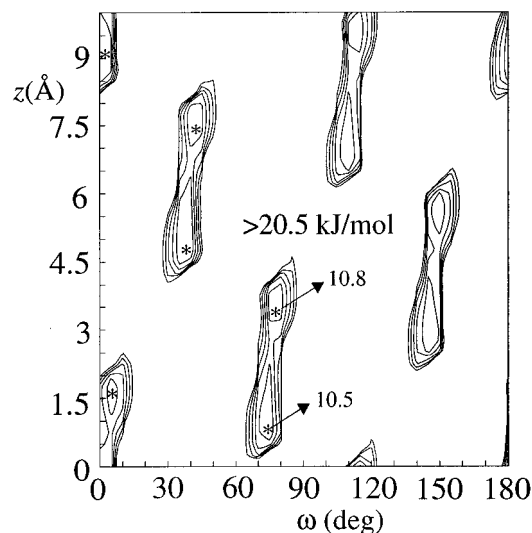


Figure 5. Map of the packing energy as a function of ω and z for the monoclinic unit cell with axes $a = 15.45$ Å, $b = 14.36$ Å, and $c = 20$ Å and with $\gamma = 116^\circ$ and space group $P2_1/a$, with the chain axis fixed at the position $x/a = y/b = 0.25$. The curves are drawn at intervals of 2 kJ/(mol of monomeric unit) with respect to the absolute minimum of the map. The absolute minimum is referred to the absolute minimum of the map of Figure 4, assumed as zero.

Figure 5, when the chain axis is in the position $x/a \approx y/b \approx 0.25$, have energies ≈ 2 kJ/(mol of monomeric unit) higher.

Calculations of the structure factors were performed for different models of packing corresponding to the different positions of the chain in the unit cell which give the energy minima present in the maps of Figures 4 and 5. A good agreement between calculated structure factors and experimental intensities, observed in the X-ray fiber diffraction pattern of Figure 1, is obtained for a model very near to that corresponding to the absolute minimum of the packing energy of the map of Figure 4 ($\omega = 179.3^\circ$, $z = 9.89$ Å, $x/a = 0.0096$, $y/b = 0.263$).

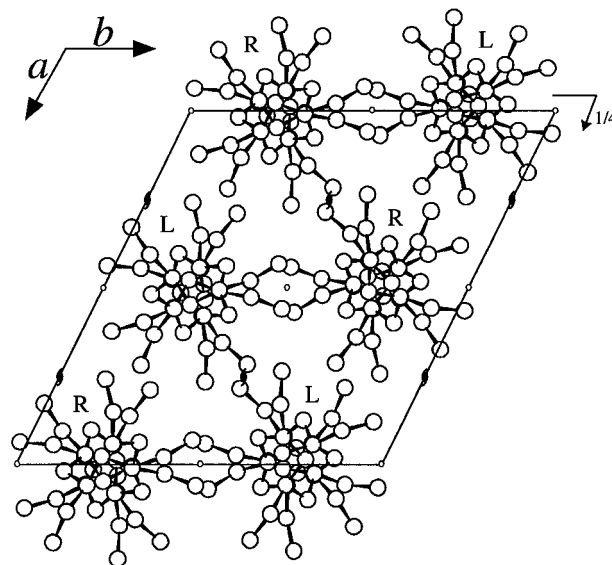


Figure 6. Model of packing of form II of s-PB in the monoclinic unit cell with axes $a = 15.45$ Å, $b = 14.36$ Å, and $c = 20$ Å with $\gamma = 116^\circ$, and space group $P2_1/a$. R = right handed helix, L = left-handed helix. The crystallographic symmetry elements of the space group $P2_1/a$ are also shown.

The model of packing of form II of s-PB that gives the best agreement is reported in Figure 6. A comparison between calculated (F_c) and observed (F_o) structure factors is reported in Table 2. A fairly good agreement is apparent; the agreement factor is $R = 16.4\%$ for all the observed reflections. The fractional coordinates of the carbon atoms of the asymmetric unit in the model of Figure 6, for the space group $P2_1/a$, are reported in Table 3.

It is apparent from the structure model of Figure 6 that the chains of form II of s-PB are packed according to a pseudohexagonal mode of packing. It is worth noting, however, that, in the model of chain conformation with complex $s(5/3)_2$ helical symmetry (Figures 3 and 6), the backbone atoms and the side group atoms are arranged along the chain in such a way as to produce an outside envelope similar to that of cylinders of radius r and R , respectively. Hence, it appears that the chains have a cylindrical outside envelope, in which hollows and bulges are periodically repeated, as it occurs in a screw.¹³ A good mode of packing for these kinds of helices (when the ratio r/R is in the range 0.3–0.8) is generally obtained in a tetragonal lattice with a coordination number equal to 4,¹³ each right-handed helix being surrounded by four left-handed helices and vice versa. Various isotactic polymers, having chains in the fourfold helical $s(4/1)$ conformation or in the complex helical $s(M/N)$ conformation, with M and N not corresponding to very small integers or with fractional ratio M/N , are crystallized in a tetragonal lattice. Some examples are form I and form III of isotactic poly(4-methyl-1-pentene) (7_2 helices and space group $P4$ or $P4b2$ for the form I,^{14–17} 4_1 helices and space group $I4_1$ for the form III^{18,19}), form II of isotactic poly(1-butene) (11_3 helices and space group $P4$),^{20,21} isotactic poly[(*R*),-(*S*)-4-methyl-1-hexene] (7_2 helices and space group $P4$),¹⁶ form I of isotactic poly(vinylcyclohexane) (4_1 helices and space group $I4_1/a$),^{22,23} isotactic poly(*o*-methylstyrene) (4_1 helices and space group $I4_1cd$),²⁴ and isotactic poly(*m*-methylstyrene) (11_3 helices and space group $P4$).²⁵ Among syndiotactic polymers, only one example has been found so far, that is syndiotactic poly(4-methyl-1-

Table 2. Comparison between Observed Structure factors F_o , Evaluated from the Intensities Observed in the X-ray Fiber Diffraction Pattern of Form II of Figure 1, and Calculated Structure Factors, F_c , for the Model of Packing of Figure 6 in the Space Group $P2_1/a$ ^a

hkl	d_{obs}^a (Å)	d_{calc}^a (Å)	F_o	F_c
210	7.56	7.68	4.1	5.2
200	6.94	6.94	31.5	29.5
{ 020 220	6.44	6.45	34.1	24.9
		6.30		23.2
210	5.07	5.23	3.6	4.7
030		4.30		3.6
220	3.92	3.94	4.1	7.2
420		3.84		7.1
{ 240 430	3.56	3.59	4.4	8.0
		3.57		7.5
211		5.06		7.7
121		4.91		11.4
321		4.78		8.8
131		4.61		7.1
{ 231 301	4.31	4.57	14.0	11.8
		4.51		4.9
031		4.21		4.7
331	4.13	4.11	14.5	11.8
221		3.87		10.0
311		3.78		7.1
421		3.77		8.5
411		3.73		7.5
312		4.56		7.6
322		4.41		6.2
232		4.25		5.8
302		4.20		6.3
032	3.99	3.95	3.9	7.3
332		3.87		4.3
312		3.60		5.3
{ 113 203 023 223	4.85	5.09	31.2	21.2
		4.81		6.0
		4.64		12.6
		4.58		16.4
313		4.07		8.0
114		4.65		6.2
114	4.33	4.22	9.8	10.5
204	4.02	4.06	11.0	11.4
{ 024 224	3.82	3.95	10.1	8.5
		3.92		4.2
214		3.61		5.2
{ 105 015 215	3.84	3.84	11.5	7.6
		3.82		15.8
		3.55		8.2

^a The Bragg distances calculated according to the unit cell with axes $a = 15.45$ Å, $b = 14.36$ Å, and $c = 20$ Å and with $\gamma = 116^\circ$ and those observed in the X-ray fiber diffraction pattern of form II of Figure 1 are also shown.

pentene), characterized by $s(12/7)2$ helical chains packed in a tetragonal lattice with space group $P4$.¹²

Exceptions to this simple rule have been found for form III of isotactic poly(1-butene), characterized by 4_1 helical chains packed in an orthorhombic lattice with space group $P2_12_12_1$,²⁶ and for isotactic poly(3-methyl-1-butene), characterized by 4_1 helical chains packed in a monoclinic lattice with space group $P2_1/b$.²⁷ For these polymers, a high symmetry tetragonal lattice would have a too low density, so the polymers are crystallized in a lattice with lower symmetry.

According to the analysis reported in this paper, form II of s-PB represents another exception to the rule of packing of chains having complex helical conformation. Although the chains of form II of s-PB have a complex $s(5/3)2$ helical conformation, they do not pack in a tetragonal lattice. Also in this case the density would be too low. The chains are packed in a monoclinic lattice (with lower symmetry) and the structure is similar to that of isotactic poly(3-methyl-1-butene),²⁷ in spite of the

Table 3. Fractional Coordinates of the Carbon Atoms of the Asymmetric Unit for the Model of Figure 6 in the Space Group $P2_1/a$

	<i>x/a</i>	<i>y/b</i>	<i>z/c</i>
1 CH ₂	-0.063	0.304	0.436
2 CH	-0.058	0.234	0.493
3 (CH ₂)side	-0.150	0.192	0.535
4 CH ₃	-0.242	0.128	0.495
5 CH ₂	0.032	0.291	0.536
6 CH	0.056	0.217	0.580
7 (CH ₂)side	0.097	0.156	0.537
8 CH ₃	0.122	0.080	0.578
9 CH ₂	0.126	0.276	0.636
10 CH	0.078	0.310	0.693
11 (CH ₂)side	0.154	0.396	0.736
12 CH ₃	0.216	0.494	0.695
13 CH ₂	0.014	0.216	0.736
14 CH	-0.057	0.238	0.780
15 (CH ₂)side	-0.139	0.242	0.737
16 CH ₃	-0.212	0.263	0.778
17 CH ₂	-0.098	0.157	0.836
18 CH	-0.025	0.174	0.893
19 (CH ₂)side	-0.056	0.075	0.935
20 CH ₃	-0.064	-0.020	0.895
21 CH ₂	-0.011	0.267	0.936
22 CH	0.080	0.306	0.980
23 (CH ₂)side	0.171	0.361	0.937
24 CH ₃	0.265	0.402	0.978
25 CH ₂	0.076	0.377	0.036
26 CH	0.006	0.317	0.093
27 (CH ₂)side	-0.020	0.391	0.136
28 CH ₃	-0.069	0.446	0.095
29 CH ₂	0.047	0.258	0.136
30 CH	-0.029	0.174	0.180
31 (CH ₂)side	-0.096	0.081	0.137
32 CH ₃	-0.174	-0.006	0.178
33 CH ₂	0.018	0.139	0.236
34 CH	0.059	0.220	0.293
35 (CH ₂)side	0.132	0.200	0.336
36 CH ₃	0.218	0.205	0.295
37 CH ₂	-0.023	0.221	0.336
38 CH	0.010	0.319	0.380
39 (CH ₂)side	0.026	0.415	0.337
40 CH ₃	0.059	0.515	0.379

different chain configuration and conformation. From the model of Figure 6 it is apparent that the chains of form II are packed according to a pseudohexagonal packing; the a and b axes of the unit cell are nearly equal (15.45 vs 14.36 Å), and γ is close to 120° ($\gamma = 116^\circ$). Each chain is surrounded by six (four enantiomorphous and two isomorphous) chains, so that the density is higher than that of an hypothetical tetragonal lattice.

It is worth noting that a mode of packing with coordination number equal to six generally occurs for polymers with chains having, in a first approximation, a form of a cylinder of uniform radius (r/R near to 1, for instance, polyethylene,²⁸ polytetrafluoroethylene,²⁹ polyisobutylene^{30,31}).

Disorder phenomena characterize often the crystal structures of isotactic polymers. Indeed, various amounts of disorder in the distribution of right- and left-handed helices, as well as of up and down chains, in the sites of the lattice can be present depending on the thermal and mechanical histories of the sample.^{13,17,19,32} For syndiotactic polymers with chains in helical $s(M/N)2$ conformations, the presence of binary axes perpendicular to the chain axis implies that up and down chains are not distinguished. Only right- and left-handed helices can be discriminated; hence, the structure of syndiotactic polymers is often characterized by disorder in the distribution of enantiomorphous helices.^{2,33,34} This kind of disorder could be present in form II of s-PB, but the

few observable X-ray diffraction data avoid examination in more detail of this aspect of the structure.

Conclusions

Oriented fiber samples of s-PB with a percentage of crystals in form II higher than that reported in a previous paper¹ are obtained by drawing at room temperature amorphous compression molded samples, just before the beginning of the crystallization in form I.

The crystal structure of form II of s-PB is determined by X-ray diffraction and packing energy calculations. Chains in helical conformation with $s(5/3)2$ symmetry are packed in a monoclinic unit cell with axes $a = 15.45$ Å, $b = 14.36$ Å, and $c = 20$ Å and with $\gamma = 116^\circ$. The crystalline density is 0.933 g/cm³ with four chains in the unit cell (40 monomeric units), and the space group is $P2_1/a$. Although chains having a conformation with complex helical symmetry are generally packed in a tetragonal lattice, the chains of form II of s-PB are packed according to a pseudohexagonal mode of packing.

The very sharp equatorial reflections indicate high coherent lengths along a and b crystallographic directions. From the broadening of 200 and 020 reflections and of the nearly meridional reflection, coherent lengths greater than 200 Å, along a and b , and of nearly 150 Å along c have been evaluated.

Acknowledgment. We thank Dr. M. Galimberti of Montell Ferrara for supplying the s-PB sample. Financial support from the "Ministero dell'Università e della Ricerca Scientifica e Tecnologica" is gratefully acknowledged.

References and Notes

- (1) De Rosa, C.; Venditto, V.; Guerra, G.; Pirozzi, B.; Corradini, P. *Macromolecules*, **1991**, *24*, 5645.
- (2) De Rosa, C.; Venditto, V.; Guerra, G.; Corradini, P. *Makromol. Chem.* **1992**, *193*, 1351.
- (3) De Rosa, C.; Guerra, G.; Grassi, A. *Macromolecules* **1996**, *29*, 471.
- (4) Ewen, J. A.; Jones, R. L.; Razavi, A.; Ferrara, J. D. *J. Am. Chem. Soc.* **1988**, *110*, 6255. Albizzati, E.; Resconi, L.; Zambelli, A. *European Patent Application* 387609 (Himont Inc.), 1991; *Chem. Abstr.* **1991**, *114*, 62980a.
- (5) Cromer, D. T.; Maan, J. B. *Acta Crystallogr.* **1968**, *A24*, 321.
- (6) Yoon, D. Y.; Sundararajan, P. R.; Flory, P. J. *Macromolecules* **1975**, *8*, 776.
- (7) Sundararajan, P. R.; Flory, P. J. *J. Am. Chem. Soc.* **1974**, *96*, 5025.
- (8) IUPAC Commission on Macromolecular Nomenclature. *Pure Appl. Chem.* **1981**, *53*, 733.
- (9) Corradini, P.; Pasquon, I. *Rend. Fis. Accad. Lincei* **1955**, *19*, 453.
- (10) Corradini, P.; Petraccone, V.; Pirozzi, B. *Eur. Polym. J.* **1976**, *12*, 831. Kusanagi, H.; Tadokoro, H.; Chatani, Y. *Macromolecules* **1976**, *9*, 531.
- (11) De Rosa, C.; Venditto, V.; Guerra, G.; Corradini, P. *Macromolecules* **1992**, *25*, 6938.
- (12) De Rosa, C.; Venditto, V.; Guerra, G.; Corradini, P. *Polymer* **1995**, *36*, 3619.
- (13) Corradini, P. In *The Stereochemistry of Macromolecules*; Ketley, A. D., Ed.; Marcel Dekker Inc.: New York, 1968; Vol. 3.
- (14) Natta, G.; Corradini, P.; Bassi, I. W. *Rend. Fis. Acc. Lincei* **1955**, *19*, 404.
- (15) Frank, F. C.; Keller, A.; O'Connor, A. *Philos. Mag.* **1959**, *8*, 200.
- (16) Bassi, I. W.; Bonsignori, O.; Lorenzi, G. P.; Pino, P.; Corradini, P.; Temussi, P. A. *J. Polym. Sci., Polym. Phys. Ed.* **1971**, *9*, 193.
- (17) Kusanagi, H.; Takase, M.; Chatani, Y.; Tadokoro, H. *J. Polym. Sci., Polym. Phys. Ed.* **1978**, *16*, 131.
- (18) De Rosa, C.; Borriello, A.; Venditto, V.; Corradini, P. *Macromolecules* **1994**, *27*, 3864.
- (19) De Rosa, C.; Auriemma, F.; Borriello, A.; Corradini, P. *Polymer* **1995**, *36*, 4723.
- (20) Turner-Jones, A. *J. Polym. Sci., Polym. Phys. Ed.* **1963**, *1*, 455.
- (21) Petraccone, V.; Pirozzi, B.; Frasci, A.; Corradini, P. *Eur. Polym. J.* **1976**, *12*, 323.
- (22) Natta, G.; Corradini, P.; Bassi, I. W. *Makromol. Chem.* **1959**, *33*, 247.
- (23) De Rosa, C.; Borriello, A.; Corradini, P. *Macromolecules* **1996**, *29*, 6323.
- (24) Corradini, P.; Ganis, P. *Nuovo Cimento Suppl.* **1960**, *15*, 96.
- (25) Corradini, P.; Ganis, P. *J. Polym. Sci., Polym. Phys. Ed.* **1960**, *43*, 311.
- (26) Cojazzi, G.; Malta, V.; Celotti, G.; Zannetti, R. *Makromol. Chem.* **1976**, *177*, 915.
- (27) Corradini, P.; Ganis, P.; Petraccone, V. *Eur. Polym. J.* **1970**, *6*, 281.
- (28) Bunn, C. W. *Trans. Faraday Soc.* **1939**, *35*, 482.
- (29) Clark, E. S.; Muus, L. T. *Z. Kristallogr.* **1962**, *117*, 119.
- (30) Liquori, A. M. *Acta Crystallogr.* **1955**, *8*, 345.
- (31) Tanaka, T.; Chatani, Y.; Tadokoro, H. *J. Polym. Sci., Polym. Phys. Ed.* **1974**, *12*, 515.
- (32) Guerra, G.; Petraccone, V.; Corradini, P.; De Rosa, C.; Napolitano, R.; Pirozzi, B.; Giunchi, G. *J. Polym. Sci., Polym. Phys. Ed.* **1984**, *22*, 1029.
- (33) De Rosa, C.; Corradini, P. *Macromolecules* **1993**, *26*, 5711.
- (34) Auriemma, F.; De Rosa, C.; Corradini, P. *Macromolecules* **1993**, *26*, 5719.

MA970133D